Carbon acquisition by *Trichodesmium*: The effect of pCO_2 and diurnal changes

Sven A. Kranz
Alfred Wegener Institute for Polar and Marine Research, Am Handelshafen 12, 27570 Bremerhaven, Germany

Dieter Sültemeyer
Fachbereich Biologie, Technische Universität Kaiserslautern, Postfach 3049, D-67653 Kaiserslautern, Germany

Klaus-Uwe Richter and Björn Rost
Alfred Wegener Institute for Polar and Marine Research, Am Handelshafen 12, 27570 Bremerhaven, Germany

Abstract

We investigated carbon acquisition by the N_2-fixing cyanobacterium *Trichodesmium* IMS101 in response to CO_2 levels of 15.1, 37.5, and 101.3 Pa (equivalent to 150, 370, and 1000 ppm). In these acclimations, growth rates as well as cellular C and N contents were measured. In vivo activities of carbonic anhydrase (CA), photosynthetic O_2 evolution, and CO_2 and HCO_3^- fluxes were measured using membrane inlet mass spectrometry and the ^{14}C disequilibrium technique. While no differences in growth rates were observed, elevated CO_2 levels caused higher C and N quotas and stimulated photosynthesis and N_2 fixation. Minimal extracellular CA (eCA) activity was observed, indicating a minor role in carbon acquisition. Rates of CO_2 uptake were small relative to total inorganic carbon (Ci) fixation, whereas HCO_3^- contributed more than 90% and varied only slightly over the light period and between CO_2 treatments. The low eCA activity and preference for HCO_3^- were verified by the ^{14}C disequilibrium technique. Regarding apparent affinities, half-saturation concentrations ($K_{1/2}$) for photosynthetic O_2 evolution and HCO_3^- uptake changed markedly over the day and with CO_2 concentration. Leakage (CO_2 efflux : Ci uptake) showed pronounced diurnal changes. Our findings do not support a direct CO_2 effect on the carboxylation efficiency of ribulose-1,5-bisphosphate carboxylase/oxygenase (RubisCO) but point to a shift in resource allocation among photosynthesis, carbon acquisition, and N_2 fixation under elevated CO_2 levels. The observed increase in photosynthesis and N_2 fixation could have potential biogeochemical implications, as it may stimulate productivity in N-limited oligotrophic regions and thus provide a negative feedback on rising atmospheric CO_2 levels.

Marine phytoplankton contribute up to 50% of global primary production (Falkowski et al. 1998) and influence Earth's climate by altering various biogeochemical cycles (Schlesinger 2005). In this respect, phytoplankton can be distinguished into so-called functional types, which affect these cycles differently. Next to diatoms (silicifiers) and coccolithophores (calcifiers), diazotrophic cyanobacteria (dinitrogen-fixers) contribute largely to overall marine primary production. The current increase in atmospheric CO_2 and rising sea-surface temperature are bound to affect phytoplankton communities in numerous ways (Boyd and Doney 2002). In view of potential ecological implications and feedbacks on climate, several studies have investigated CO_2 sensitivity in key phytoplankton species, mainly focusing on the groups of diatoms and coccolithophores (Nielsen 1995; Burkhardt and Riebesell 1997; Rost et al. 2003).

Diazotrophic cyanobacteria affect marine ecosystems by providing reactive nitrogen to otherwise nitrogen-limited regions. The filamentous nonheterocystous cyanobacterium *Trichodesmium* thrives in oligotrophic areas of tropical and subtropical seas. Forming large blooms, this species contributes about half of all marine N_2 fixation (Mahaffey et al. 2005). In contrast to other diazotrophs, *Trichodesmium* has evolved special features allowing N_2 fixation to occur during the photoperiod. To protect the oxygen-sensitive enzyme nitrogenase, which catalyzes the reduction of N_2 to NH_3, from photosynthetic O_2 evolution, this species has developed distinct diurnal rhythms in photosynthesis and N_2 fixation (Berman-Frank et al. 2001*b*). This intriguing species has been investigated by several studies focusing on the effects of phosphorus and iron limitations as well as temperature, salinity, and irradiance (Berman-Frank et al. 2001*a*; Fu and Bell 2003; Breitbarth et al. 2007). The potential influence of CO_2-induced changes in seawater chemistry, however, has been ignored until very recently.

Barcelos e Ramos et al. (2007), Levitan et al. (2007), and Hutchins et al. (2007) observed a strong increase in photosynthesis and N_2 fixation in *Trichodesmium* under elevated CO_2 levels. This trend is predominantly attributed to changes in cell division (Hutchins et al. 2007; Levitan et al. 2007) but also altered elemental ratios of carbon to nitrogen (Levitan et al. 2007) or nitrogen to phosphorus (Barcelos e Ramos et al. 2007). Despite differences in their findings, e.g., in terms of absolute rates or elemental ratios,

Acknowledgments

We thank Ilana Berman-Frank, Orly Levitan, Katherina Petrou, and two anonymous reviewers for their constructive comments on the manuscript. The research leading to these results has received funding from the European Research Council under the European Community's Seventh Framework Programme (FP7/2007-2013)/ERC grant agreement (205150).

the magnitudes of these CO_2 effects exceed those previously seen in other marine photoautotrophs. The underlying processes responsible for the strong CO_2 sensitivity in this important diazotroph are currently unknown.

Understanding CO_2 sensitivity in photosynthesis, which provides the energy for growth and any other downstream processes, requires information about modes of carbon uptake and fixation in phytoplankton. Most of the reductive power and energy generated in the light reactions of photosynthesis are allocated for assimilation of inorganic carbon (Ci) and subsequent reduction (Falkowski and Raven 2007). A large proportion of these costs is associated with the operation of so-called CO_2 concentrating mechanisms (CCMs), which function to increase the carboxylation reaction of ribulose-1,5-bisphosphate carboxylase/oxygenase (RubisCO). This enzyme evolved during times of elevated CO_2 levels and is characterized by very low affinity for its substrate CO_2, a slow maximum turnover rate, as well as a susceptibility to a competing reaction with O_2. Since cyanobacterial RubisCO has one of the highest half-saturation constants ever measured (K_M of 105–185 μmol L^{-1} CO_2; Badger et al. 1998), this group has to invest considerable resources into the CCM to avoid the risk of carbon limitation as well as the wasteful process of photorespiration. This CCM involves active uptake of CO_2 and/or HCO_3^- as well as carbonic anhydrase (CA), which catalyzes the otherwise slow conversion between HCO_3^- and CO_2. Processes that minimize the CO_2 efflux from the cell are also important components of an efficient CCM. To date, there are no physiological studies on these central processes in *Trichodesmium*.

In the present study, we investigated the physiological responses of *Trichodesmium* IMS101 to different CO_2 levels, comparing Last Glacial Maximum (15.1 Pa), present-day (37.5 Pa), and projected upper CO_2 values for the year 2100 (101.3 Pa; Raupach et al. 2007). To assess diurnal changes in these treatments, responses were generally measured at different time intervals over the photoperiod. In each CO_2 treatment, responses in growth rates, elemental ratios, and rates of photosynthesis and production of particulate organic nitrogen were measured. To develop a process-based understanding of responses in the incubations, different in vivo bioassays were applied. O_2 evolution under steady-state photosynthesis, quantified CO_2 and HCO_3^- uptake rates, as well as cellular leakage (CO_2 efflux : Ci uptake) were measured by the use of a membrane inlet mass spectrometer. Activities of external carbonic anhydrase (eCA) were determined by monitoring ^{18}O exchange from doubly labelled $^{13}C^{18}O_2$. As a second approach, short-term ^{14}C disequilibrium measurements were conducted to estimate CA activities and distinguish the carbon source taken up.

Methods

Culture conditions—Stock cultures of *Trichodesmium erythraeum* IMS101 (isolated by Prufert-Bebout et al. 1993) were grown at 25°C in a 12 : 12 h light : dark (LD) cycle at 150 μmol photons m^{-2} s^{-1} in 0.2-μm-filtered unbuffered YBCII media (Chen et al. 1996). For experiments, semicontinuous batch cultures were grown in 1-liter custom-made cylinder flasks (diameter 7 cm) at the same temperature and light regime. Air containing three different CO_2 partial pressures (pCO_2) of 15.1, 37.5, and 101.3 Pa (equivalent to 150, 370, and 1000 ppm) was sparged continuously through the cultures. CO_2 gas mixtures were generated with gas-mixing pumps (Digamix 5KA18/8-F and 5KA36/8-F, Woesthoff GmbH), using CO_2-free air (Nitrox CO_2RP280; Domnick Hunter GmbH), pure CO_2 (Air Liquide Deutschland GmbH), or ambient air. Regular dilution with fresh, pre-acclimated media ensured that the carbonate chemistry remained constant and that the cells stayed in the midexponential growth phase. Cultures in which the pH had shifted in comparison to cell-free media at the respective pCO_2 (pH drift >0.06) were excluded from further analysis. Total alkalinity was measured in duplicate by potentiometric titration and calculated from linear Gran Plots (Gran 1952). The carbonate system was calculated from total alkalinity (TA), pCO_2, phosphate, temperature, and salinity using the program CO2Sys (Lewis and Wallace 1998). Equilibrium constants of Mehrbach et al. (1973) refitted by Dickson and Millero (1987) were chosen. Carbonate chemistry for the respective pCO_2 treatments is given in Table 1.

Table 1. Parameters of the seawater carbonate system calculated from pCO_2, alkalinity, pH, phosphate, temperature, and salinity using the CO2Sys program (Lewis and Wallace 1998) (n=3; ±SD).

pCO_2 (Pa)	pH (NBS)	CO_2 (μmol L^{-1})	DIC (μmol L^{-1})	TA (μEq L^{-1})
15.1	8.56±0.03	3.9±0.3	1879±24	2535±12
37.5	8.26±0.03	9.9±0.7	2113±20	2535±12
101.3	7.89±0.03	27.2±1.9	2322±16	2535±12

Growth, elemental composition, and fixation rates—Cultures were acclimated to the respective pCO_2 for at least 14 d (>5 generations) before measuring. In general, samples were taken at the beginning of the photoperiod to account for diurnal changes. Cell densities were determined using an inverted microscope (Zeiss, Axiovert 200) by measuring the number of filaments, length, and cell size in a Sedgwick-Rafter Cell (S50, Graticules). The average cell size for each pCO_2 treatment was estimated based on the length of individual filaments and corresponding cell counts (>10,000 individual counts). Samples for chlorophyll *a* (Chl *a*) measurements were filtered onto cellulose nitrate filters (Sartorius) and stored at −80°C. Chl *a* was subsequently extracted in 5–10 mL acetone (overnight in darkness, at 4°C) and determined with a fluorometer (Turner Designs).

Samples for particulate organic carbon (POC) and nitrogen (PON) were filtered onto precombusted (500°C; 9 h) GFF filters and stored in precombusted (500°C; 9 h) petri dishes at −20°C. Prior to analysis, filters were treated with 200 μL HCl (0.1 μmol L^{-1}) to remove all inorganic carbon. POC and PON were subsequently measured in duplicate on an EA mass spectrometer (ANCA-SL 2020).

Growth rates were determined based on changes in cell density, Chl *a* concentration, as well as POC and PON, respectively, and are given as mean values. Growth rates (μ) were calculated as:

$$\mu(\mathrm{d}^{-1}) = \frac{\ln(N_1) - \ln(N_0)}{\Delta t} \quad (1)$$

where N_0 and N_1 are concentration of cells, Chl *a*, POC, or PON at time t_0 and t_1, respectively, and Δt is the time between sampling intervals. Production rates of PON (P_N) and POC (P_C) per day were calculated according to the following equations:

$$P_N = \mu \times \mathrm{PON} \times (\mathrm{Chl}\ a)^{-1} \quad (2)$$

$$P_C = \mu \times \mathrm{POC} \times (\mathrm{Chl}\ a)^{-1} \quad (3)$$

Determination of CA activity—After a minimum of 14 d acclimation to the respective pCO_2, cells were concentrated by gentle filtration over a membrane filter (pore size 8 μm; Isopore, Millipore). The culture media was stepwise exchanged with the respective assay medium, and CA activities were determined using a membrane inlet mass spectrometer (MIMS). The system consisted of a temperature-controlled cuvette, a membrane-inlet (polytetrafluoroethylene membrane, 0.01 mm), and a sectorfield multicollector mass spectrometer (Isoprime; GV Instruments). Gas molecules dissolved in solution permeated through the membrane and were ionized, and, depending on their mass : charge ratio (*m*/*z*), ions were then separated and detected.

CA activity was determined from the ^{18}O depletion of doubly labelled $^{13}C^{18}O_2$ in water caused by several hydration and dehydration steps of CO_2 and HCO_3^- (Silverman 1982). The reaction sequence of ^{18}O loss from initial $^{13}C^{18}O^{18}O$ (m/z = 49) via the intermediate $^{13}C^{18}O^{16}O$ (m/z = 47) to the final isotopomer $^{13}C^{16}O^{16}O$ (m/z = 45) was recorded simultaneously. The ^{18}O enrichment was calculated as:

$$\log(\text{enrichment}) = \log\frac{(^{13}C^{18}O_2) \times 100}{^{13}C^{16}O_2 + {}^{13}C^{18}O^{16}O + {}^{13}C^{18}O_2} = \log\frac{(m/z\,49) \times 100}{(m/z\,45) + (m/z\,47) + (m/z\,49)} \quad (4)$$

CA measurements were performed in 8 mL of YBCII medium buffered with 2-(4-[2-hydroxyethyl]-1-piperazinyl)ethanesulfonic acid (HEPES, 50 mmol L^{-1}, pH 8.00) at 25°C. If not stated otherwise, all measurements were carried out in the dark to avoid interference with light-dependent carbon uptake by the cells. Bicarbonate was added (1 mmol L^{-1} $NaH^{13}C^{18}O$), and once the chemical equilibrium was reached, the uncatalyzed rate of ^{18}O loss was recorded for at least 5 min. Subsequently, 100–200 μL of concentrated cell suspension were added to the media to yield a final Chl *a* concentration of 0.5–2.5 μg mL^{-1}. For calculation of extracellular CA activities (eCA), the increasing rate of ^{18}O depletion after addition of the cells (S_2) was compared to the uncatalyzed reaction (S_1) and normalized on a Chl *a* basis (Badger and Price 1989):

$$U = \frac{(S_2 - S_1) \times 100}{S_1 \times \mu\mathrm{g\ Chl}\ a} \quad (5)$$

Consequently, 100 units (U) correspond to an enhancement in the interconversion between HCO_3^- and CO_2 relative to the spontaneous rate by 100% per μg Chl *a*. Following the eCA measurements, light was added (300 μmol photons m^{-2} s^{-1}) to monitor light-induced changes in the ^{18}O exchange. This method is indicative of active transport of Ci, as there will be an enhanced influx of labelled Ci into the cell to the active site of internal CA, resulting in an increase of the ^{18}O loss (Badger and Price 1989).

Intracellular CA (iCA) activity was determined in the presence of 50 μmol L^{-1} dextran-bound sulfonamide (DBS), a membrane-impermeable inhibitor of eCA. The activity of iCA was estimated from the rapid decline in log (enrichment) upon the injection of cells, defined as Δ, and calculated according to Palmqvist et al. (1994). Values of Δ are expressed per μg Chl *a*.

Determination of photosynthesis and Ci fluxes—The O_2 and Ci fluxes were determined during steady-state photosynthesis with the same MIMS as for the CA measurements. The method established by Badger et al. (1994) is based on simultaneous measurements of O_2 and CO_2 during consecutive light and dark intervals. Known amounts of inorganic carbon were added to measure photosynthesis and carbon uptake rates as a function of CO_2, HCO_3^-, or dissolved inorganic carbon (DIC) concentrations. Photosynthesis, CO_2 uptake, and HCO_3^- uptake were calculated according to the equations of Badger et al. (1994). Cells were harvested in the same manner as for the CA measurements using CO_2-free YBCII medium (50 mmol L^{-1} HEPES, pH 8.00) and transferred into the cuvette before DBS was added (final concentration of 50 μmol L^{-1}). Light and dark intervals during the assay lasted 6 and 5 min, respectively. The incident photon flux density was 300 μmol photons m^{-2} s^{-1}. Chl *a* concentrations in the assay ranged from about 0.5 to 4 μg mL^{-1}. Further details on the method and calculations are given in Badger et al. (1994) and Rost et al. (2007).

^{14}C disequilibrium method—Cells were concentrated via gentle filtration in the same manner as for the MIMS assays, but they were washed and resuspended with buffered YBCII media (BICINE-NaOH, 20 mmol L^{-1}, pH 8.50). Afterward, cells were transferred into a cuvette (4 mL volume) and pre-incubated to 300 μmol photons m^{-2} s^{-1} for 6 min. The ^{14}C disequilibrium technique makes use of the transient isotopic disequilibrium upon an acidic ^{14}C spike into cell suspension at high pH to determine whether CO_2 or HCO_3^- is the preferred carbon species for photosynthesis (Espie and Colman 1986; Elzenga et al. 2000). This approach also provides semi-quantitative estimates of external CA activity. In the

present study, we followed the protocol described by Rost et al. (2007).

Results

Growth, elemental ratios, and fixation rates—To assess the overall sensitivity of *Trichodesmium* to different CO_2 levels (15.1, 37.5, and 101.3 Pa), responses in growth rates, elemental ratios, rates of photosynthesis, and production rates of particulate organic nitrogen were measured. Growth rates were determined during mid-exponential growth phase based on cell counts, Chl *a*, POC, and PON. The mean growth rate was 0.31 ± 0.04 d^{-1} (Fig. 1a) and did not differ significantly between pCO_2 treatments ($p = 0.378$; one way ANOVA). The C : N ratios (4.6 ± 0.1) and Chl *a* : cell ratios (1.0 ± 0.2) did not differ between the treatments. However, POC and PON increased from 4.1 ± 0.6 pmol C $cell^{-1}$ and 0.9 ± 0.1 pmol N $cell^{-1}$ at 37.5 Pa to 5.4 ± 0.6 pmol C $cell^{-1}$ and 1.2 ± 0.1 pmol N $cell^{-1}$ at 101.3 Pa CO_2 (Figs. 1b,c). The corresponding POC and PON production rates increased from 51.7 ± 8.0 to 67.6 ± 7.4 μmol C (mg Chl *a*)$^{-1}$ h^{-1} and from 11.4 ± 2.2 to 14.9 ± 1.8 μmol N (mg Chl *a*)$^{-1}$ h^{-1}, representing a stimulation in carbon and nitrogen fixation by almost 40%.

In terms of diurnal changes, carbon and nitrogen contents per cell showed distinct patterns leading to strong changes in C : N ratios (Fig. 2a). During the course of the day, the C : N ratio increased from 4.76 ± 0.04 at the onset of the photoperiod to 4.91 ± 0.04 around midday (09:00 h–12:00 h). It decreased to 4.48 ± 0.08 during the afternoon (12:00 h–17:00 h) and subsequently increased to 4.95 ± 0.09 toward the scotoperiod (21:00 h). This diurnal variation in the C : N ratio indicates distinct differences in the patterns of carbon or nitrogen fixation over the day. Rates of photosynthesis and respiration (based on O_2 evolution) as determined by MIMS also showed pronounced diurnal changes in all acclimations (Fig. 2b). Rates of photosynthesis decreased by 48% during the first 3 h of the photoperiod, while dark respiration increased by 102%. After reaching lowest and highest rates around midday, respectively, this pattern reversed, and photosynthesis increased while dark respiration decreased toward the end of the photoperiod (Fig. 2b).

Carbonic anhydrase activities—External CA activity determined by MIMS directly reflects the acceleration in the conversion between CO_2 and HCO_3^- relative to the spontaneous rate. In *Trichodesmium*, eCA activities were about 50 ± 10 units (μg Chl *a*)$^{-1}$, and they neither varied between treatments nor over the photoperiod (data not shown). The activity of internal CA remained constant in all acclimations and was near the detection limit, i.e., Δ values were about 0.25 ± 0.08 (μg Chl *a*)$^{-1}$ following calculations of Palmqvist et al. (1994).

The ^{18}O exchange technique can provide information about active Ci transport systems. As shown in Fig. 3, illumination resulted in an enhanced uptake of ^{18}O-labelled $^{13}CO_2$ (*m*/*z* 49 and 47) and a large efflux of unlabelled $^{13}CO_2$ (*m*/*z* 45), leading to a light-dependent decrease in log (enrichment). Similar patterns were observed in all acclimations and throughout the photoperiod.

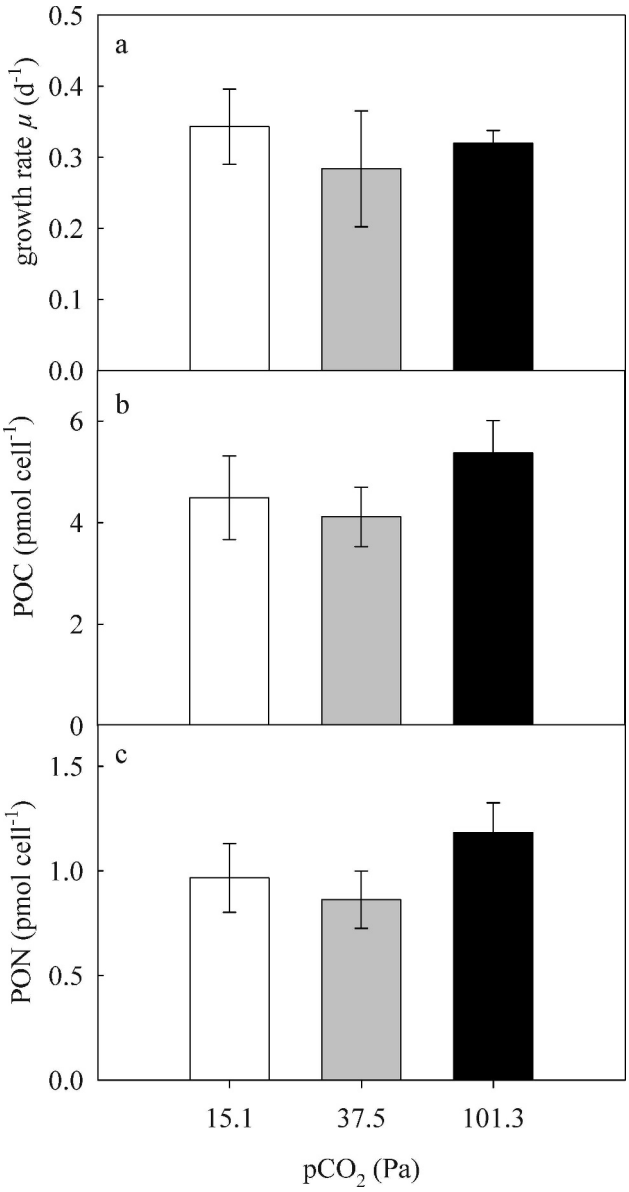

Fig. 1. (a) Mean growth rates of *Trichodesmium* based on changes in cell density, Chl *a*, POC, PON (b) content of POC per cell, and (c) content of PON per cell in different acclimations of 15.1 Pa, 37.5 Pa, and 101.3 Pa pCO_2. Data present mean values ($n \geq 3$; ±SD).

Photosynthetic O_2 evolution and carbon fluxes—Photosynthesis and Ci uptake are shown as functions of CO_2 and HCO_3^- concentration measured during steady-state conditions (Fig. 4) by MIMS. Maximum rates of photosynthesis (V_{max}) and half-saturation concentrations ($K_{1/2}$) were obtained from a Michaelis–Menten fit and are summarized for all pCO_2 treatments in Table 2. Kinetics for photosynthetic O_2 evolution were affected both by pCO_2 and photoperiod. While V_{max} differed only slightly between pCO_2 treatments, diurnal variations were pronounced

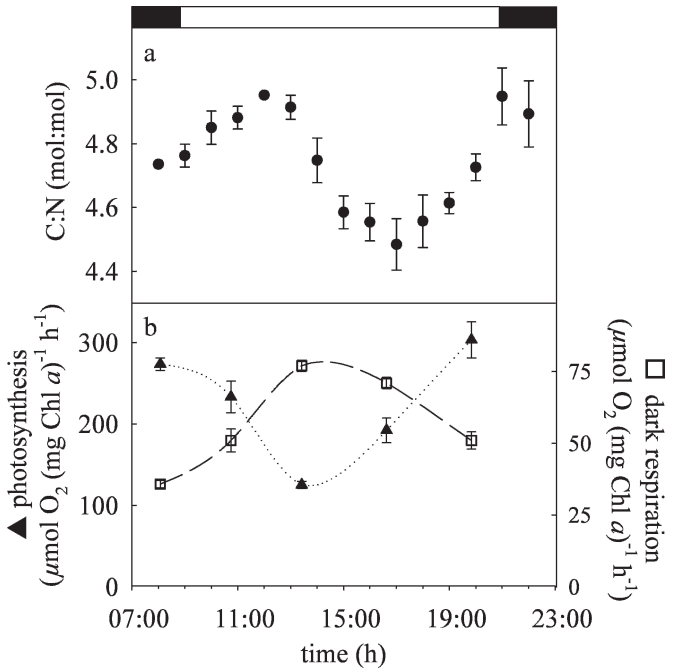

Fig. 2. (a) Diurnal variations in C : N ratios of the 37.5 Pa acclimation in *Trichodesmium*. Symbols represent average values ($n \geq 2 \pm$ SD). (b) Pattern of photosynthesis and dark respiration as measured during carbon flux measurements in light and dark cycles, respectively. Data present mean values ($n \geq 3$; $\pm$SD).

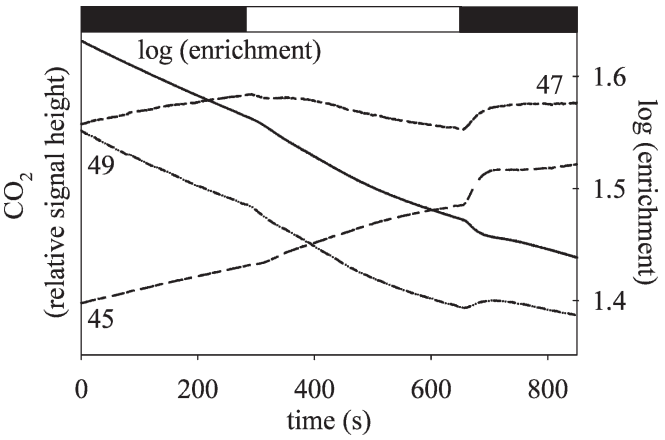

Fig. 3. Time course of changes in log (enrichment) and the CO_2 isotopomers $^{13}C^{18}O_2$ (*m*/*z* 49), $^{13}C^{16}O^{18}O$ (*m*/*z* 47), $^{13}C^{16}O_2$ (*m*/*z* 45) by cells of *Trichodesmium* acclimated to 37.5 Pa CO_2 measured at 15:00 h. The eCA inhibitor DBS (50 mmol L^{-1}) was applied during the assay. Black and white bars at the top indicate the dark and light period, respectively.

(Fig. 5a; Table 2). Minimum values were obtained about 3 h after illumination (125 to 170 μmol O_2 [mg Chl *a*]$^{-1}$ h^{-1}), and increased by nearly twofold toward the end of the photoperiod (303 to 330 μmol O_2 [mg Chl *a*]$^{-1}$ h^{-1}). As indicated by the $K_{1/2}$ (DIC) values, affinities differed significantly between pCO_2 acclimations and also showed a strong diurnal pattern, with highest values around midday (Fig. 5b; Table 2). $K_{1/2}$ (CO_2) values for photosynthesis ranged between 0.9 and 13.6 μmol L^{-1} CO_2 (data not shown).

In terms of carbon fluxes, *Trichodesmium* showed a preference for HCO_3^- as a carbon source for photosynthesis (Fig. 4; Table 3). The high HCO_3^- contribution to net fixation was verified by the ^{14}C disequilibrium method (*see* below). The $K_{1/2}$ values for HCO_3^- uptake and diurnal variability therein strongly increased from low to the high pCO_2 acclimation (Table 2), ranging between 40 and 100 μmol DIC L^{-1} in the low pCO_2 treatment and 85 and 520 μmol DIC L^{-1} in the high pCO_2 treatment. This CO_2 effect on affinities persisted despite the large diurnal variations in $K_{1/2}$, being most pronounced during midday and lowest at the beginning of the photoperiod. Rates for CO_2 uptake were very low in all acclimations and throughout the photoperiod (Table 2). In terms of gross CO_2 uptake, $K_{1/2}$ and V_{max} remained unaffected by pCO_2 in the acclimation as well as over the photoperiod. $K_{1/2}$ values ranged between 3.3 and 6.1 μmol L^{-1} CO_2, and V_{max} ranged between 51 and 114 μmol CO_2 (mg Chl *a*)$^{-1}$ h^{-1}. Net CO_2 flux was often negative, showing lowest values between 12:00 h and 15:00 h, which made it impossible to calculate $K_{1/2}$ values. These rates reflect the CO_2 efflux that occurs during steady-state photosynthesis. The proportion of Ci efflux compared to gross Ci uptake, i.e., cellular leakage, was estimated by MIMS from the CO_2 efflux observed directly upon darkening. Independent of the pCO_2 acclimation, *Trichodesmium* showed large variations in leakage during the photoperiod, and the highest ratio (~0.5) occurred at 12:00 h (Fig. 6).

^{14}C disequilibrium method—Figure 7 shows an example of the ^{14}C incorporation of a culture acclimated to 101.3 Pa CO_2. Monitoring the ^{14}C incorporation for more than 12 min, i.e., well into equilibrium, yielded a high level of precision for determining the carbon sources. In measurements of the same culture without DBS (control), similar rates of ^{14}C incorporation were obtained, indicating a lack of significant eCA activity. The ratio of HCO_3^- to net fixation did not significantly differ between the acclimations or throughout the photoperiod; values ranged between 0.86 and 0.95 (Table 3).

Discussion

This study assessed the sensitivity of *Trichodesmium erythraeum* (IMS101) to changes in CO_2 concentration by measuring responses to the different acclimations (e.g., growth, elemental ratios, fixation rates) and by describing the modes of carbon acquisition (e.g., CA activities, O_2 evolution, carbon fluxes). Cells were acclimated in unbuffered artificial seawater and maintained at low cell densities to match the natural environment in nonbloom situations as closely as possible. *Trichodesmium* showed no responses in growth rate, but particulate organic carbon and nitrogen production rates increased strongly at elevated pCO_2 (Fig. 1) The apparent $K_{1/2}$ values for photosynthetic O_2 evolution were significantly lower than values known for RubisCO (Badger et al. 1998), demonstrating the operation of a CCM in this species. *Trichodesmium* showed a strong

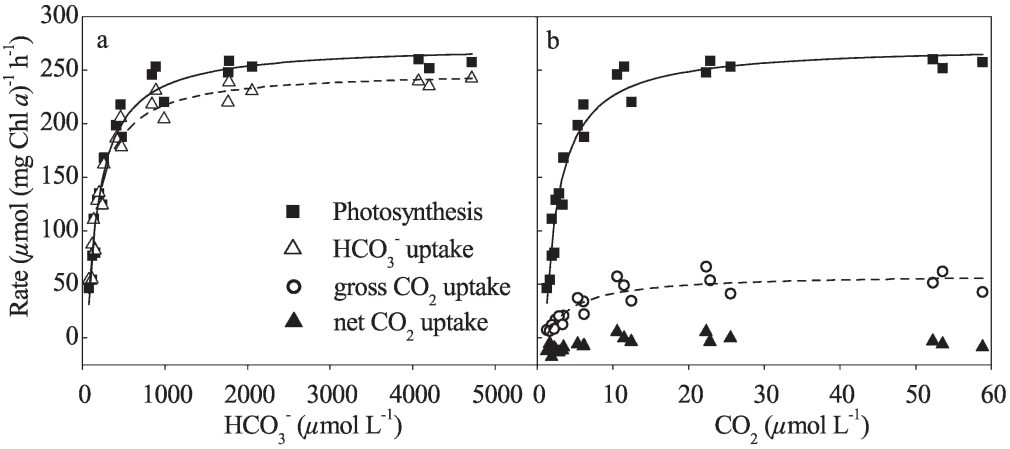

Fig. 4. Chl *a*–specific rates of (a) photosynthesis and HCO_3^- uptake and (b) photosynthesis and gross as well as net CO_2 uptake and as a function of HCO_3^- and CO_2 concentration in the assay media. The given examples show results from cells acclimated to 101.3 Pa CO_2 and were measured at 07:00 h. Curves were obtained from a Michaelis–Menten fit.

preference for HCO_3^- as a carbon source, which did not change with CO_2 availability or over the diurnal cycle. In terms of CO_2 and HCO_3^- affinities, however, cells showed strong responses to CO_2 treatments and photoperiod.

Growth, elemental ratios, and production rates—Previous studies have observed CO_2 effects on growth (Riebesell et al. 1993), photosynthesis (Nielsen 1995; Rost et al. 2003), and elemental ratios (Burkhardt and Riebesell 1997) in diatoms and coccolithophores. Large responses in growth, photosynthesis, and elemental ratios with respect to changes in pCO_2 have recently been found in the diazotrophic species *Trichodesmium* (Barcelos e Ramos et al. 2007; Hutchins et al. 2007; Levitan et al. 2007). It should be noted that all these studies, including the present one, have used the same *Trichodesmium* isolate from the Atlantic Ocean (IMS101).

Our findings indicate no sensitivity in growth rates over the tested CO_2 range (15.1 to 101.3 Pa CO_2), but they do show CO_2-dependent changes in the elemental composition of *Trichodesmium* (Fig. 1a). In comparison to the previously published data, growth rates (μ = 0.32) are slightly higher than those obtained by Levitan et al. (2007; μ = 0.27) and lower than those from Barcelos e Ramos et al. (2007; μ = 0.45) under high CO_2. For low CO_2 levels, our data do not agree with the diminished rates observed by Levitan et al. (2007; μ = 0.12) and Barcelos e Ramos et al. (2007; μ = 0.15 to 0.3) or the absence of growth observed by Hutchins et al. (2007). According to the latter study, *Trichodesmium* cannot thrive under the CO_2 levels that

Table 2. $K_{1/2}$ and V_{max} of photosynthesis, HCO_3^- uptake, and gross CO_2 uptake over a diurnal cycle and acclimated to 15.1, 37.5, and 101.3 Pa pCO_2. The photoperiod started at 09:00 h and ended at 21:00 h. Kinetic parameters were calculated from a Michaelis–Menten fit to the combined data of several ($n \geq 3$; ±SD) independent measurements. Values for $K_{1/2}$ and V_{max} are given in μmol L^{-1} and μmol (mg Chl *a*)$^{-1}$ h^{-1}, respectively.

		Photosynthesis		HCO_3^- uptake		Gross CO_2 uptake	
Time (h)	pCO_2 (Pa)	$K_{1/2}$ (DIC)	V_{max} (DIC)	$K_{1/2}$ (HCO_3^-)	V_{max} (HCO_3^-)	$K_{1/2}$ (CO_2)	V_{max} (CO_2)
07:00	15.1	61±24	233±14	63±25	242±15	4±1	88±7
	37.5	126±13	219±7	111±9	213±4	6±1	56±3
	101.3	214±18	274±8	190±16	250±7	5±1	60±5
09:30	15.1	40±11	187±9	41±11	232±11	4±1	82±7
	37.5	72±12	207±6	27±8	219±9	4±1	73±6
	101.3	85±33	233±20	52±23	226±18	6±2	56±6
12:00	15.1	102±33	147±9	30±6	199±6	3±2	67±10
	37.5	286±96	171±16	112±29	198±11	4±1	60±3
	101.3	519±54	125±4	111±23	150±7	7±1	51±2
15:00	15.1	54±12	298±12	25±6	266±9	3±1	90±8
	37.5	94±29	270±20	51±11	232±9	3±1	97±10
	101.3	443±105	192±15	188±38	206±10	5±1	64±2
18:00	15.1	25±35	319±21	30±8	248±9	4±1	92±4
	37.5	112±25	330±16	61±15	284±13	4±2	114±13
	101.3	257±70	303±22	181±56	274±20	5±1	90±7

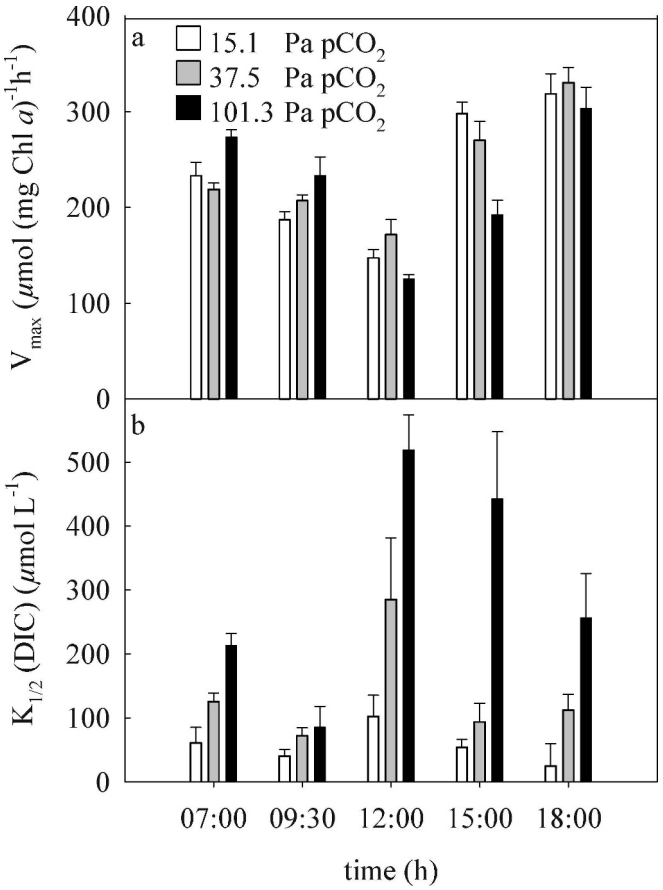

Fig. 5. Maximum rates (V_{max}) and half-saturation concentrations ($K_{1/2}$) of photosynthesis over a diurnal cycle acclimated to different pCO_2 conditions. Kinetic parameters were calculated from a Michaelis–Menten fit to the combined data of several independent measurements. Error bars denote ±SD.

Table 3. Contribution of HCO_3^- uptake relative to net C fixation. Values of MIMS measurement were obtained at 2 mmol L^{-1} DIC. Values of ^{14}C were obtained by fitting the ^{14}C incorporation pattern. Values represent the mean of three independent measurements ($n \geq 3$; ±SD).

		HCO_3^- uptake : C fixation	
Time (h)	pCO_2 (Pa)	MIMS	^{14}C disequilibrium
07:00	15.1	1.02±0.20	–
	37.5	1.01±0.08	–
	101.3	0.98±0.11	0.94±0.01
09:30	15.1	1.08±0.28	0.94±0.01
	37.5	1.02±0.19	0.95±0.01
	101.3	1.02±0.22	0.92±0.01
12:00	15.1	1.11±0.35	0.93±0.01
	37.5	1.09±0.31	0.93±0.01
	101.3	1.13±0.38	0.90±0.01
15:00	15.1	0.99±0.19	0.92±0.02
	37.5	0.98±0.15	0.93±0.01
	101.3	1.06±0.27	0.87±0.02
18:00	15.1	0.99±0.17	–
	37.5	1.01±0.24	–
	101.3	1.02±0.35	0.92±0.02

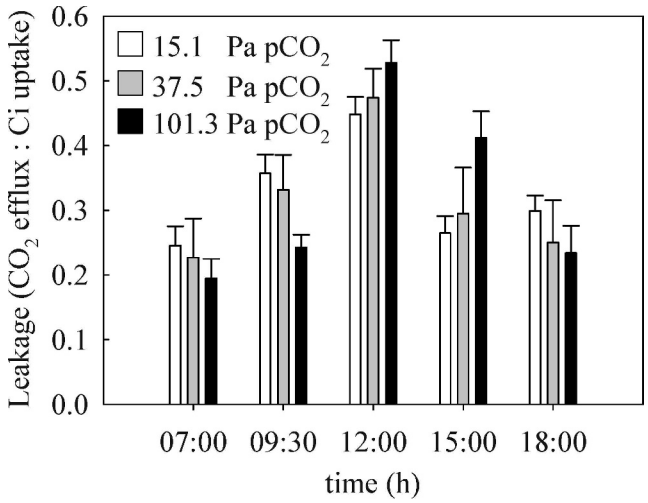

Fig. 6. Ratio of CO_2 efflux : gross Ci uptake in *Trichodesmium* at different acclimations over a day. Values indicate leakage measured with MIMS method calculated for the CO_2 concentrations in the acclimation. Data present mean values ($n \geq 3$; ±SD).

prevailed during glacial times and commonly occur under bloom conditions. Some of the strong CO_2 dependence observed by Barcelos e Ramos et al (2007) is also caused by reduced growth rates in the low pCO_2 range, which furthermore shows significant variability.

The carbon and nitrogen contents per cell increased at high pCO_2 compared to the lower pCO_2 acclimations (Figs. 1b,c) while the C : N ratios remained constant at ~4.6 (obtained at the beginning of the photoperiod). Measured carbon quotas and elemental ratios are comparable with those obtained by Hutchins et al. (2007) and similar to C : N ratios reported for the low pCO_2 acclimation by Barcelos e Ramos et al. (2007). However, in their study, the cell quotas for C and N decreased with increasing pCO_2, which is the opposite to the trend

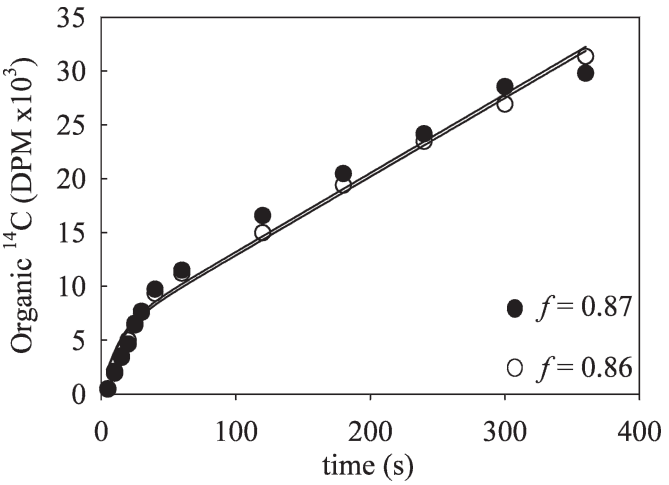

Fig. 7. Examples of disintegrations per minute (DPM) of ^{14}C during a short-term incubation of cells acclimated to 101.3 Pa CO_2 and measured at 15:00 h. Values of f in DBS-treated cells (closed symbols) and the control (open symbols) represent the proportion of HCO_3^- uptake relative to net C fixation.

observed by Levitan et al. (2007), who found an increase in C and N quota as well as the respective ratio under elevated pCO_2. In all studies, the observed magnitude in CO_2 sensitivity to carbon and N_2 fixation differed strongly. Using the acetylene reduction assay, Barcelos e Ramos et al. (2007) and Levitan et al. (2007) observed stimulation in N_2 fixation by approximately 40% and even up to 400%, while Hutchins et al. (2007) obtained stimulation by up to 35% over the respective CO_2 range. In our study, we assessed the process of N_2 fixation by measuring the production of particulate organic nitrogen. The results show a 40% increase in the production rates under high pCO_2 (Fig. 1c) as well as elevated C fixation (Fig. 1b). Both processes were equally stimulated, which is reflected by the constant C : N ratios. These findings are consistent with Barcelos e Ramos et al. (2007) and Hutchins et al. (2007), while in Levitan et al. (2007), C : N ratios increased with CO_2.

The discrepancy between studies may be attributed to differences in methodology (e.g., midexponential growth versus late stationary phase) or growth conditions (light intensities). Preliminary data (S. Kranz and O. Levitan unpubl. data) showed that light levels strongly influenced CO_2 dependency of growth as well as C and N quotas in *Trichodesmium*. Responses consistent within all mentioned studies on *Trichodesmium* show that elevated CO_2 stimulates both C and N_2 fixation rates

Diurnal variations in photosynthesis and N_2 fixation—Diazotrophic organisms have developed numerous strategies to fix N_2 efficiently (Berman-Frank et al. 2007). Nitrogenase, the enzyme that catalyzes the reduction of atmospheric N_2 to ammonia, is inhibited by O_2, and thus N_2 fixation has to be separated from photosynthetic O_2 evolution. In the nonheterocystous *Trichodesmium*, a distinct diurnal pattern of N_2 fixation and O_2 evolution has been observed (Berman-Frank et al. 2001*b*; Milligan et al. 2007). Our study verifies these diurnal rhythms, finding a pronounced decrease in photosynthesis and increased dark respiration during midday (Fig. 2b). The concomitant decrease in C : N ratio during that time also reflects increasing rates of N_2 fixation (Fig. 2a). Additionally, the Mehler reaction appears to be involved in light-dependent O_2 uptake during N_2 fixation (Kana 1993; Milligan et al. 2007). The inverse correlation between photosynthesis and respiration observed in the present and previous studies is caused by the fact that both processes share the same protein complex in the electron transport chain. Consequently, the increase in dark respiration results in a down-regulation of the water splitting in Photosystem II (PSII) due to a negative feedback reaction in the electron transport chain (Milligan et al. 2007).

Due to high adenosine triphosphate (ATP) and electron requirements, N_2 fixation is among the most costly processes for the cell next to carbon assimilation (Falkowski and Raven 2007). However, this process occurs during midday when photosynthesis is down-regulated and hence the ATP and nicotinamide adenine dinucleotide phosphate (NADPH) supply is low. The way in which *Trichodesmium* copes with this shortage in energy supply is not yet fully understood. Another enigma relates to CO_2 sensitivity in photosynthetic carbon assimilation and N_2 fixation, as both processes compete for ATP and reductants provided by the light reaction of photosynthesis. While external CO_2 levels could affect the C fixation directly by controlling the carboxylation efficiency of RubisCO or indirectly by modifying the energy costs of their CCM, there are currently no CO_2-related processes known to directly influence nitrogenase activities. The strong effects of CO_2 as well as diurnal changes in C and N fixation observed in this and previous studies must be reflected in the modes of carbon acquisition of *Trichodesmium*. In the following, we will characterize the CCM of *Trichodesmium*, the diurnal changes, and regulation with respect to CO_2 availability.

Carbonic anhydrase activities—External CA (eCA), which accelerates the interconversion between HCO_3^- and CO_2 at the cell surface, has been found to increase in response to decreasing CO_2 supply in various microalgal species (Berman-Frank et al. 1995; Rost et al. 2003). It is a common notion that eCA is involved in indirect HCO_3^- utilization by converting HCO_3^- to CO_2, which could then diffuse into the cell or be actively transported through the plasma membrane and subsequently used for photosynthesis (Sültemeyer et al. 1998; Elzenga et al. 2000). External CA activity in *Trichodesmium* was low—values of about 50 units per μg Chl *a*—and did not change with CO_2 supply (data not shown). In species that express significant quantities of eCA, activity is usually an order of magnitude higher (Rost et al. 2003; Trimborn et al. 2008). Moreover, there was no stimulation of photosynthesis by the addition of bovine CA (data not shown). The lack of significant eCA activity was further verified by the ^{14}C disequilibrium method (Elzenga et al. 2000), which yielded similar ^{14}C incorporation patterns in the presence and absence of DBS (Fig. 7). Consequently, the low activity and the lack of induction under low CO_2 supply indicate that eCA does not play an important, if any, role in the carbon acquisition by *Trichodesmium*.

Internal carbonic anhydrase (iCA) in cyanobacteria is required for the rapid conversion from HCO_3^- to CO_2 prior to the fixation by RubisCO. When interpreting iCA activity, as defined according to Palmqvist et al. (1994), one has to bear in mind that Δ values are in vivo estimates, which depend not only on the rate of intracellular ^{18}O depletion (i.e., CA activity) but also on the diffusive influx of doubly labelled CO_2 and, thus, on the diffusive properties of cyanobacterial membranes and cell shape. Therefore, despite being semiquantitative estimates, Δ values are still appropriate for direct comparison between treatments within the same species. Internal CA in *Trichodesmium* is presumably located in the carboxysome to operate near RubisCO (Price et al. 2008). These data show that *Trichodesmium* possesses low iCA activity, which is constitutively expressed. The iCA activity observed, despite being low, possibly reflects the CA activity inside the carboxysome catalyzing the interconversion between HCO_3^- and CO_2 (Price et al. 2008). In addition, the CO_2 uptake system in *Trichodesmium*, located

at the thylakoid membrane, functions like CA by accelerating the conversion of CO_2 into HCO_3^- (Price et al. 2008). However, this function may only play a role under illumination when electrons and NAD(P)H are available to drive this process.

Using the ^{18}O exchange technique, we examined the presence of light-dependent Ci transport systems. In the case of active Ci uptake, a decline in log (enrichment) during illumination would be expected as a result of an enhanced uptake of ^{18}O-labelled CO_2 and HCO_3^- into the cells, increased ^{18}O exchange catalyzed by internal CA, and subsequent efflux of ^{18}O-unlabelled CO_2 (Badger and Price 1989; Palmqvist et al. 1994). Such a net CO_2 efflux from photosynthetically active cells can only be explained by an active accumulation of Ci and the presence of iCA within the cells. As shown in Fig. 3, illumination resulted in a decrease of $^{13}C^{18}O_2$ ($m/z = 49$) due to uptake of labelled carbon species and an increase in $^{13}C^{16}O_2$ ($m/z = 45$) as a result of efflux of the latter. The consequent decrease in log (enrichment) was accompanied by an increase in oxygen production (data not shown). These patterns were measured in all acclimations throughout the photoperiod and are indicative of the presence of a CCM.

Photosynthetic O_2 evolution—Early studies demonstrated a CO_2-dependent regulation of the CCM of cyanobacteria (Kaplan et al. 1980). More recent studies have shown that the apparent affinity for Ci increases strongly with decreasing Ci availability in the culture medium (Woodger et al. 2003; Price et al. 2004). These studies typically compared present-day (i.e., ~37.5 Pa) with unnaturally high CO_2 levels (i.e., 2000–5000 Pa), and it is therefore not yet fully understood to what extent this regulation occurs under environmentally relevant CO_2 concentrations. In the present study, photosynthetic O_2 evolution as a function of CO_2 concentration was monitored to gain information about the overall efficiency and regulation of carbon acquisition in *Trichodesmium*. Half-saturation constants were generally lower (0.9–13.6 μmol L^{-1} CO_2) than those reported for cyanobacterial RubisCO (105–185 μmol L^{-1} CO_2; Badger et al. 1998). Moreover, we observed a gradual regulation by pCO_2 in the acclimations. While we obtained lowest apparent affinities for Ci at high pCO_2, maximum photosynthetic O_2 evolution rates were not affected in the bioassays (Fig. 5a; Table 2). The high apparent affinities, as well as the CO_2-dependent changes therein, demonstrate the operation of a CCM for *Trichodesmium*, and these findings are consistent with kinetics observed in other cyanobacteria (Sültemeyer 1998; Price et al. 2004).

The strongest variation in the CCM was, however, observed over the diurnal cycle. As an example, $K_{1/2}$ for photosynthetic O_2 evolution varied between 85 and 520 μmol L^{-1} DIC in the 101.3 Pa CO_2 treatment (Fig. 6b). This up- and down-regulation of the CCM is most likely associated with the diurnal pattern of N_2 fixation. During midday, when N_2 fixation is greatest, the apparent affinities as well as maximum rates for photosynthetic O_2 evolution are down-regulated. The down-regulation of the CCM and the up-regulation of dark- and light-dependent respiration (*see* previous discussion) result in lower net O_2 evolution, which is a prerequisite for efficient N_2 fixation, as shown previously (Berman-Frank et al. 2001*b*; Milligan et al. 2007). The trigger for this diurnal CCM regulation may be changes in the redox state of the photosynthetic electron chain, which could result from lower PSII activity in line with higher respiration in *Trichodesmium* and/or the concentration of photorespiratory metabolites (Kaplan et al. 2001).

Although the CO_2 dependence of O_2 evolution provides information about the efficiency and regulation of carbon acquisition, it cannot provide any details about the underlying mechanisms. To get a process-based understanding, we therefore have to look at the carbon source(s) and respective uptake kinetics.

Carbon source and uptake kinetics—An essential component of a CCM is the active uptake of inorganic carbon and its accumulation within the cell. Several methods have been employed to distinguish between CO_2 and HCO_3^- uptake in microalgae and cyanobacteria. In this study, estimates of CO_2 and HCO_3^- uptake were obtained by means of mass spectrometry (Badger et al. 1994) and the ^{14}C disequilibrium technique (Espie and Colman 1986; Elzenga et al. 2000). This is the first time such techniques have been applied to *Trichodesmium*.

Rates of CO_2 uptake determined by MIMS were very low in *Trichodesmium*, representing generally less than 10% relative to net carbon fixation (Table 2). Net CO_2 fluxes were low, even negative under some conditions, reflecting higher CO_2 efflux than uptake. Since the CO_2 uptake could not support the observed rates of photosynthesis, most of the inorganic carbon was taken up as HCO_3^- (Table 3). In the instances when net fluxes of CO_2 were negative, HCO_3^- uptake exceeded net fixation (Badger et al. 1994). The strong preference for HCO_3^- in *Trichodesmium* did not change with CO_2 treatments or photoperiod. These findings were confirmed by the ^{14}C disequilibrium method (Espie and Colman 1986; Elzenga et al. 2000), which showed on average 92% contribution of HCO_3^- uptake relative to net carbon fixation. Please note that the contribution of HCO_3^-, as determined by ^{14}C disequilibrium approach, can never exceed net fixation (Elzenga et al. 2000). These results are consistent with previous studies showing that CCMs in cyanobacteria are generally based on active HCO_3^- uptake (Price et al. 2008). With respect to the high accumulation of Ci necessary to compensate for their low-affinity RubisCO, cyanobacteria may prefer HCO_3^- over CO_2 because of the higher equilibrium concentration of HCO_3^- in marine systems. Moreover, as a charged molecule, HCO_3^- can be accumulated more efficiently in the cytoplasm than CO_2 (Price and Badger 1989).

The apparent affinities of the HCO_3^- uptake systems differed among CO_2 treatments and over the photoperiod. With decreasing CO_2 availability, apparent affinity for HCO_3^- uptake increased (Table 2), and this trend generally persisted throughout the photoperiod. Various studies have shown that changes in apparent affinity can be accomplished by expression of high versus low affinity transporters (Omata et al. 1999; Price et al. 2004) or by post-translational modifications of existing transport proteins,

e.g., by phosphorylation (Sültemeyer et al. 1998). For *Trichodesmium*, deoxyribonucleic acid (DNA) sequence analysis indicates the presence of one medium and/or low affinity HCO_3^- transporter (BicA) and a low-affinity NDH-1_4 CO_2 uptake system (Price et al. 2004, 2008). The observed $K_{1/2}$ values for HCO_3^- uptake and the low contribution of CO_2 to the overall uptake observed in our study support the findings from these molecular studies.

The uptake kinetics for HCO_3^- varied strongly over the photoperiod, although they were less pronounced than variations in photosynthetic O_2 evolution (Table 2). Apparent affinities for HCO_3^- were highest at the beginning of the photoperiod, with $K_{1/2}$ values between ~25 and 50 μmol L^{-1} HCO_3^-, and lowest during and following N_2 fixation, with $K_{1/2}$ values up to 190 μmol L^{-1} HCO_3^-. These diurnal variations in HCO_3^- transport efficiency occurred in all treatments but were more distinct under high pCO_2.

Changes in uptake kinetics, as in the HCO_3^- uptake system, may be caused by variations in the reductive state of photosynthetic electron transport carriers, which affect the balance between cyclic and linear electron transport and thus the energy supply for transporters (Li and Canvin 1998). With respect to diurnal changes in *Trichodesmium*, the electron flow can also be altered by the up-regulation of the Mehler reaction (Kana 1993; Milligan et al. 2007). As an O_2-consuming process, it can additionally effect the $[O_2]:[CO_2]$ ratio in the proximity of RubisCO, which has been suggested to be another trigger for the regulation of CCMs (Kaplan et al. 2001). Consequently, changes in the redox state of the photosynthetic electron transport carriers as well as the low $[O_2]:[CO_2]$ ratios during midday could have contributed to the observed down-regulation of the HCO_3^- uptake efficiency. The highly induced HCO_3^- uptake systems at the beginning of the photoperiod may have been triggered by light and the excess of electrons. An up-regulated CCM and consequently efficient Calvin cycle provides the best mechanism to drain electrons (photochemical quenching) and avoid photodamage, similar to the response observed in *Chlamydomonas reinhardtii* (Marcus et al. 1986). The frequently excessive HCO_3^- uptake observed may further provide a means to efficiently dissipate excess light energy (Tchernov et al. 1997). These and possibly other quenching mechanisms are important for *Trichodesmium*, since it thrives in low latitudes close to the surface, with high average irradiance.

Leakage—The efficiency of a CCM not only depends on the kinetics of the active carbon uptake systems but also on the loss of Ci via efflux. Leakage (ratio of Ci efflux to total Ci uptake) will increase the energetic costs of a CCM and/or decrease its capability to reach carbon saturation (Raven and Lucas 1985). Consequently, to increase the overall CCM efficiency, it is necessary to minimize the leakage. Following the approach by Badger et al. (1994), the MIMS was used to estimate leakage.

The MIMS approach yielded similar estimates for leakage in all pCO_2 treatments, yet the photoperiod imposed strong changes in leakage, with values as high as 0.55 during midday (Fig. 6). These high values were the result of increasing efflux combined with the down-regulation of total Ci uptake (Fig. 5; Table 2). As argued already, such high leakage might help to dissipate excess energy at times when PSII and Calvin cycle activity are down-regulated in *Trichodesmium*. Such modification of leakage will most likely be associated with a CO_2-trapping mechanism. It has been suggested that CO_2 efflux from the carboxysome is converted back to HCO_3^- by the PSII-associated NDH-CO_2 uptake system (Price et al. 2008). The diurnal changes in PSII activity (Berman-Frank et al. 2001*b*) may therefore directly regulate the effective leakage of the cell and thus explain most of the diurnal variation we observed in *Trichodesmium*. It should be noted, however, that the CO_2 efflux estimated according to Badger et al. (1994) is based on the assumptions that the rate of diffusive CO_2 efflux in the light is well represented by the first seconds upon darkening. Despite shortcomings in methodology, our data indicate that higher leakage, for instance during midday, reflect a down-regulation of the overall CCM activity, which is consistent with the lower affinities of the Ci uptake system during these times (Table 2; Fig. 5).

Ecological and biogeochemical implications—Diazotrophic cyanobacteria like *Trichodesmium* support a large fraction of biological productivity in tropical and subtropical areas and exert, over long timescales, a significant influence on global carbon cycles by providing a major source of reactive N to the water column (Falkowski and Raven 2007). Despite its global importance, studies have only recently begun to investigate the effect of elevated CO_2 on species such as *Trichodesmium* (Barcelos e Ramos et al. 2007; Hutchins et al. 2007; Levitan et al. 2007). This study, consistent with previous investigations, showed a strong increase in photosynthesis and N_2 fixation under elevated CO_2 levels. To the extent that we can extrapolate these laboratory experiments to the real ocean, the marine N_2 fixation by *Trichodesmium* could increase from present-day to future pCO_2 level by 40% (the present study) or even up to 400% (Levitan et al. 2007). Similarly, high sensitivity to changes in carbonate chemistry has been observed in photosynthesis (Barcelos e Ramos et al. 2007; Hutchins et al. 2007; Levitan et al. 2007; present study).The magnitude of these CO_2 effects would, if representative for the natural environment, have large implications for the future ocean.

The relevance of marine N_2 fixation is also expected to increase owing to the projected expansion of oligotrophic regions to higher latitudes as a result of surface ocean warming and increased stratification (Boyd and Doney 2002; Breitbarth et al. 2007). Elevated N_2 fixation in a future ocean will likely influence phytoplankton in terms of productivity and species composition, and thereby alter the microbial food web (Mulholland et al. 2006). In summary, CO_2-related effects on photosynthesis and N_2 fixation as well as the overall changes in the ecosystem would provide a negative feedback on the increase in atmospheric CO_2. Significant uncertainties remain, however, as to the degree of sensitivity to CO_2 and the modification of these responses by other environmental factors (e.g., P or Fe limitation). Moreover, it is still unknown whether the

observed responses in *Trichodesmium* can be generalized to include other important diazotrophic cyanobacteria.

The present study has taken a first step toward understanding the underlying processes behind strong CO_2 sensitivity by photosynthesis and N_2 fixation in *Trichodesmium*. This diazotrophic organism was found to operate an efficient CCM based almost entirely on direct HCO_3^- uptake. Consequently, a direct effect of elevated CO_2 on RubisCO carboxylation efficiency is unlikely (i.e., higher active or diffusive CO_2 uptake would increase internal CO_2/O_2 concentrations) or at least not the main reason for the CO_2 sensitivity observed. Instead, owing to the observed plasticity in CCM regulation, *Trichodesmium* may be able to optimize the allocation of resources (e.g., ATP and NADPH) between the CCM and other processes like N_2 fixation. Such a resource allocation would explain the influence of CO_2 on nitrogenase activity. In view of the potential ecological and biogeochemical implications, investigation into the regulation of photosynthesis, CCMs, and N_2 fixation in *Trichodesmium* and other important diazotrophs is clearly a research priority.

References

Badger, M. R., T. J. Andrews, S. M. Whitney, M. Ludwig, D. C. Yellowlees, W. Leggat, and G. D. Price. 1998. The diversity and coevolution of Rubisco, plastids, pyrenoids, and chloroplast-based CO_2-concentrating mechanisms in algae. Can. J. Bot. **76:** 1052–1071.

———, K. Palmqvist, and J.-W. Yu. 1994. Measurement of CO_2 and HCO_3^- fluxes in cyanobacteria and microalgae during steady-state photosynthesis. Physiol. Plant. **90:** 529–536.

———, and G. D. Price. 1989. Carbonic anhydrase activity associated with the cyanobacterium *Synechococcus* PCC7942. Plant Physiol. **89:** 51–60.

Barcelos e Ramos, J., H. Biswas, K. G. Schulz, J. La Roche, and U. Riebesell. 2007. Effect of rising atmospheric carbon dioxide on the marine nitrogen fixer *Trichodesmium*, Glob. Biogeochem. Cy. **21:** GB2028, doi:10.1029/2006GB002898.

Berman-Frank, I., J. T. Cullen, Y. Shaked, R. M. Sherrell, and P. G. Falkowski. 2001a. Iron availability, cellular iron quotas and nitrogen fixation in *Trichodesmium*. Limnol. Oceanogr. **46:** 1249–1260.

———, A. Kaplan, T. Zohary, and Z. Dubinsky. 1995. Carbonic anhydrase activity in a natural bloom forming dinoflagellate. J. Phycol. **31:** 906–913.

———, P. Lundgren, Y. Chen, H. Küpper, Z. Kolber, B. Bergman, and P. G. Falkowski. 2001b. Segregation of nitrogen fixation and oxygenic photosynthesis in the marine cyanobacterium *Trichodesmium*. Science **294:** 1534–1537.

———, A. Quigg, Z. V. Finkel, A. J. Irwin, and L. Haramaty. 2007. Nitrogen-fixation strategies and Fe requirements in cyanobacteria. Limnol. Oceanogr. **52:** 2260–2269.

Boyd, P. W., and S. C. Doney. 2002. Modelling regional responses by marine pelagic ecosystems to global climate change. Geophys. Res. Let. **29:** 1806, doi:10.1029/2001GL014130.

Breitbarth, E., A. Oschlies, and J. La Roche. 2007. Physiological constraints on the global distribution of *Trichodesmium*—effect of temperature on diazotrophy. Biogeosciences **4:** 53–61.

Burkhardt, S., and U. Riebesell. 1997. CO_2 availability affects elemental composition (C : N : P) of the marine diatom *Skeletonema costatum*. Marine Ecology Progress Series **155:** 67–76.

Chen, Y. B., J. P. Zehr, and M. Mellon. 1996. Growth and nitrogen fixation of the diazotropic filamentous nonheterocystous cyanobacterium *Trichodesmium* sp. IMS101 in defined media: Evidence for a circadian rhythm. J. Phycol. **32:** 916–923.

Dickson, A. G., and F. J. Millero. 1987. A comparison of the equilibrium constants for the dissociation of carbonic acid in seawater media. Deep-Sea Res. **34:** 1733–1743.

Elzenga, J. T. M., H. B. A. Prins, and J. Stefels. 2000. The role of extracellular carbonic anhydrase activity in inorganic carbon utilization of *Phaeocystis globosa* (Prymnesiophyceae): A comparison with other marine algae using the isotope disequilibrium technique. Limnol. Oceanogr. **45:** 372–380.

Espie, G. S., and B. Colman. 1986. Inorganic carbon uptake during photosynthesis. A theoretical analysis using the isotope disequilibrium technique. Plant Physiol. **80:** 863–869.

Falkowski, P. G., R. Barber, and V. Smetacek. 1998. Biogeochemical controls and feedbacks on ocean primary production. Science **281:** 200–206.

———, and J. A. Raven. 2007. Aquatic photosynthesis. Blackwell.

Fu, F. X., and P. R. F. Bell. 2003. Effect of salinity on growth, pigmentation, N_2-fixation and alkaline phosphatase activity of cultured *Trichodesmium* sp. Mar. Ecol. Prog. Ser. **257:** 69–76.

Gran, G. 1952. Determinations of the equivalence point in potentiometric titrations of seawater with hydrochloric acid. Oceanol. Acta **5:** 209–218.

Hutchins, D. A., F.-X. Fu, Y. Zhang, M. E. Warner, Y. Feng, K. Portune, P. W. Bernhardt, and M. R. Mulholland. 2007. CO_2 control of *Trichodesmium* N_2 fixation, photosynthesis, growth rates and elemental ratios: Implications for past, present and future ocean biogeochemistry. Limnol. Oceanogr. **52:** 1293–1304.

Kana, T. M. 1993. Rapid oxygen cycling in *Trichodesmium thiebautii*. Limnol. Oceanogr. **38:** 18–24.

Kaplan, A., M. R. Badger, and J. A. Berry. 1980. Photosynthesis and the intracellular inorganic carbon pool in the blue green alga *Anabaena variabilis*: Response to external CO_2 concentration. Planta **149:** 219–226.

———, Y. Helman, D. Tchernov, and L. Reinhold. 2001. Acclimation of photosynthetic microorganisms to changing ambient CO_2 concentration. Proc. Natl. Acad. Sci. USA **98:** 4817–4818.

Levitan, O., G. Rosenberg, I. Setlik, E. Setlikova, J. Grigel, J. Klepetar, O. Prasil, and I. Berman-Frank. 2007. Elevated CO_2 enhances nitrogen fixation and growth in the marine cyanobacterium *Trichodesmium*. Global Change Biol. **13:** 531–538.

Lewis, E., and D. W. R. Wallace. 1998. Program developed for CO_2 system calculations. ORNL/CDIAC-105. Carbon Dioxide Information Analysis Center, Oak Ridge National Laboratory, U.S. Dept. Energy.

Li, Q. L., and D. T. Canvin. 1998. Energy sources for HCO_3^- and CO_2 transport in air-grown cells of *Synechococcus* UTEX 625. Plant Physiol. **116:** 1125–1132.

Mahaffey, C., A. F. Michaels, and D. G. Capone. 2005. The conundrum of marine N_2 fixation. Am. J. Sci. **305:** 546–595.

Marcus, Y., G. Schuster, S. Michaels, and A. Kaplan. 1986. Adaptation to CO_2 level and changes in the phosphorylation of thylakoid proteins during the cell cycle of *Chlamydomonas reinhardtii*. Plant Physiol. **80:** 604–607.

Mehrbach, C., C. Culberson, J. Hawley, and R. Pytkovicz. 1973. Measurement of the apparent dissociation constants of carbonic acid in seawater at atmospheric pressure. Limnol. Oceanogr. **18:** 897–907.

Milligan, A. J., I. Berman-Frank, Y. Gerchman, G. C. Dismukes, and P. G. Falkowski. 2007. Light-dependent oxygen consumption in nitrogen-fixing cyanobacteria plays a key role in nitrogenase protection. J. Phycol. **43:** 845–852.

Mulholland, M. R., C. A. Heil, D. A. Bronk, and M. O. O'Neil. 2006. Nitrogen fixation and release of fixed nitrogen by *Trichodesmium* sp. in the Gulf of Mexico. Limnol. Oceanogr. **51:** 1762–1776.

Nielsen, M. V. 1995. Photosynthetic characteristics of the coccolithophorid *Emiliania huxleyi* (Prymnesiophyceae) exposed to elevated concentrations of dissolved inorganic carbon. J. Phycol. **31:** 715–719.

Omata, T., G. D. Price, M. R. Badger, M. Okamura, S. Gohta, and T. I. Ogawa. 1999. Identification of an ATP-binding cassette transporter involved in bicarbonate uptake in the cyanobacterium *Synechococcus* sp. strain PCC 7942. Proc. Natl. Acad. Sci. USA **96:** 13571–13576.

Palmqvist, K., J.-W. Yu, and M. R. Badger. 1994. Carbonic anhydrase activity and inorganic carbon fluxes in low- and high-Ci cells of *Chlamydomonas reinhardtii* and *Scenedesmus obliquus*. Physiologia Plantarum **90:** 537–547.

Price, G. D., and M. R. Badger. 1989. Expression of human carbonic anhydrase in the cyanobacterium *Synechococcus* PCC7942 creates a high CO_2–requiring phenotype: Evidence for a central role for carboxysomes in the CO_2-concentrating-mechanism. Plant Physiol. **91:** 505–513.

———, M. R. Badger, F. J. Woodger, and B. M. Long. 2008. Advances in understanding the cyanobacterial CO_2-concentrating-mechanism (CCM): Functional components, Ci transporters, diversity, genetic regulation and prospects for engineering into plants. J. Exp. Bot. **59:** 1441–1461.

———, F. J. Woodger, M. R. Badger, S. M. Howitt, and L. Tucker. 2004. Identification of a SulP-type bicarbonate transporter in marine cyanobacteria. Proc. Natl. Acad. Sci. USA **101:** 18228–18233.

Prufert-Bebout, L., H. W. Paerl, and C. Larsen. 1993. Growth, nitrogen fixation, and spectral attenuation in cultivated *Trichodesmium* species. Appl. Environ. Microbiol. **59:** 1367–1375.

Raupach, M. R., G. Marland, P. Ciais, C. Le Quéré, J. G. Canadell, G. Klepper, and C. B. Field. 2007. Global and regional drivers of accelerating CO_2 emissions. Proc. Natl. Acad. Sci. USA **104:** 10288–10293, doi:10.1073/pnas.0700609104.

Raven, J. A., and W. J. Lucas. 1985. Energy costs of carbon acquisition, p. 305–324. *In* W. J. Lucas and J. A. Berry [eds.], Inorganic carbon uptake by aquatic photosynthetic organisms. American Society of Plant Physiologists.

Riebesell, U., D. A. Wolf-Gladrow, and V. Smetacek. 1993. Carbon dioxide limitation of marine phytoplankton growth rates. Nature **361:** 249–251.

Rost, B., S. A. Kranz, K.-U. Richter, and P. Tortell. 2007. Isotope disequilibrium and mass spectrometric studies of inorganic carbon acquisition by phytoplankton. Limnol. Oceanogr. Methods **5:** 328–337.

———, U. Riebesell, S. Burkhardt, and D. Sültemeyer. 2003. Carbon acquisition of bloom-forming marine phytoplankton. Limnol. Oceanogr. **48:** 55–67.

Schlesinger, W. H. 2005. Biogeochemistry. Elsevier.

Silverman, D. N. 1982. Carbonic anhydrase. Oxygen-18 exchange catalyzed by an enzyme with rate contributing proton-transfer steps. Methods Enzymol. **87:** 732–752.

Sültemeyer, D. 1998. Carbonic anhydrase in eukaryotic algae: Characterization, regulation, and possible function during photosynthesis. Can. J. Bot. **76:** 962–972.

———, B. Klughammer, M. R. Badger, and G. D. Price. 1998. Protein phosphorylation and its possible involvement in the induction of the high-affinity CO_2-concentrating mechanism in cyanobacteria. Can. J. Bot. **76:** 954–961.

Tchernov, D., M. Hassidim, B. Luz, A. Sukenik, L. Reinhold, and A. Kaplan. 1997. Sustained net CO_2 evolution during photosynthesis by marine microorganisms. Curr. Biol. **7:** 723–728.

Trimborn, S., N. Lundholm, S. Thoms, K.-U. Richter, B. Krock, P. J. Hansen, and B. Rost. 2008. Inorganic carbon acquisition in potentially toxic and non-toxic diatoms: The effect of pH-induced changes in the seawater carbonate chemistry. Physiologia Plantarum **133:** 92–105, doi:10.1111/j.1399-3054.2007.01038.x.

Woodger, F. J., M. R. Badger, and G. D. Price. 2003. Inorganic carbon limitation induces transcripts encoding components of the CO_2-concentrating mechanism in *Synechococcus* sp. PCC7942 through a redox-independent pathway. Plant Physiol. **133:** 2069–2080.

Edited by: John Albert Raven

Received: 23 June 2008
Amended: 04 December 2008
Accepted: 05 December 2008